Adsorption of Eu(III) onto TiO$_2$: Effect of pH, concentration, ionic strength and soil fulvic acid

Xiaoli Tan [a,b,*], Ming Fang [c], Jiaxing Li [a], Yi Lu [a], Xiangke Wang [a,b,*]

[a] *Key Lab of New Thin Film Solar Cells, Institute of Plasma Physics, Chinese Academy of Sciences, P.O. Box 1126, Hefei, 230031 Anhui, PR China*
[b] *School of Nuclear Science and Engineering, North China Electric Power University, Beijing, 102206, PR China*
[c] *Institute of Solid States Physics, Chinese Academy of Sciences, P.O. Box 1129, Hefei, 230031 Anhui, PR China*

ABSTRACT

The effects of pH, initial Eu(III) concentration, ionic strength and fulvic acid (FA) on the adsorption of Eu(III) on TiO$_2$ are investigated by using batch techniques. The results indicate that the presence of FA strongly enhances the adsorption of Eu(III) on TiO$_2$ at low pH values. Besides, the adsorption of Eu(III) on TiO$_2$ is significantly dependent on pH values and independent of ionic strength. The adsorption of Eu(III) on TiO$_2$ is attributed to inner-sphere surface complexation. The diffuse layer model (DLM) is applied to simulate the adsorption data, and fits the experimental data well with the aid of FITEQL 3.2. X-ray photoelectron spectroscopy (XPS) is performed to study the species of Eu(III) adsorbed on the surfaces of TiO$_2$/FA–TiO$_2$ hybrids at a molecular level, which suggest that FA act as "bridge" between Eu(III) and TiO$_2$ particles to enhance the ability to adsorb Eu(III) in solution.

© 2009 Elsevier B.V. All rights reserved.

1. Introduction

In the context of safety of nuclear waste repositories as well as for the assessment of radionuclide mobility in the environment, the interaction among lanthanides/actinides, oxides and humic substances (HSs) has become a main subject of various studies. Adsorption behavior of radionuclides to minerals is a major process controlling the physicochemical behavior of radionuclides in the environment. Therefore, the knowledge of radionuclide adsorption is of great importance in the management of radioactive wastes containing long-lived actinides and lanthanides. Eu(III) is a trivalent lanthanide and a chemical homologue of trivalent actinides as both trivalent lanthanides and actinides exhibit similar adsorption properties. Adsorption of Eu(III) on hydrous metal-oxides and minerals has been studied extensively [1–15]. It was found that the adsorption of Eu(III) on minerals was strongly dependent on pH values and the adsorption of Eu(III) increased with increasing pH value. A positive effect of HSs on the adsorption of Eu(III) at low pH value and a negative effect at high pH value were found [3,4]. Different surface complexation models (SCMs) were applied to fit the experimental data, to interpret and to appraise the surface adsorption processes under different experimental conditions [6–10]. The interaction of Eu(III) and minerals was studied by using extended

X-ray adsorption fine structure (EXAFS) and time resolved laser fluorescence spectroscopy (TRLFS), which allow to clarify the uptake mechanism of trace elements by minerals [11–15]. A comprehensive understanding of the underlying physicochemical process is necessary for the evaluation of long-term performance assessment of a nuclear waste repository.

Humic substances are the major fraction of dissolved organic compounds present in surface water and soils. The high carbon content ($\sim$50–60%) of both aliphatic and aromatic character and rich in oxygen-containing functional groups (such as carboxy, phenolic, alcoholic and quinoid groups) make HSs are the primary metal-complexing chelate and hence perform a vital influence on the environmental fate, bioavailability, toxicity and mobility of heavy metal ions [16,17]. Therefore, it is important to study the adsorption and complexation of metal ions to HS–mineral hybrids, especially to study the interactions between long-lived actinides/lanthanides and HS–mineral hybrids [1–4,16].

TiO$_2$ is an ideal adsorbent for studying the effect of the surface functional groups on adsorption. Its solubility is negligible and the point of zero charge (pH$_{pzc}$) at neutral pH value makes it possible to study the adsorption of metal ions on TiO$_2$ over a broad range of pH and ionic strength [18]. Lots of recent publications have been focused on the adsorption of metal ions (such as Cu, Mo, Co, Cr, Pb, Th, Pu) by TiO$_2$ in aqueous solution to study the adsorption capacities, mechanisms, process parameters and so on [18–25]. Kim et al. [19] studied the adsorption of Cu on anatase-type TiO$_2$ and found that the adsorption of Cu increased rapidly with increasing pH value

* Corresponding authors. Tel.: +86 551 5591368; fax: +86 551 5591310.
E-mail addresses: tanxl@ipp.ac.cn (X. Tan), xkwang@ipp.ac.cn (X. Wang).

from 2 to 5 and maintained high level over pH 5. Adsorption of Mo on hydrous TiO_2 (anatase) particles indicated that the maximum adsorption appeared in the acidic pH range at low surface loading and the Langmuir model described the adsorption behavior well [21]. Results of Cr(VI) adsorption on TiO_2 in the presence of humic acid (HA) indicated that the adsorption capacity of TiO_2 was greatly influenced by the presence of HA [23]. The presence of Cr(VI) inhibited the adsorption of HA on TiO_2, leading to the decreased adsorption capacity of HA on TiO_2 with increasing Cr(VI) concentration. Adsorption of Th(IV) on TiO_2 indicated a reversible formation of an inner-sphere complex with strong pH dependence [18]. Adsorption of Pu(VI) on TiO_2 was ionic strength independent, and inner-sphere complex was considered to be formed at TiO_2 surface [25]. Although the adsorption of metal ions on TiO_2 has been extensively studied, the investigations on the adsorption of Eu(III) on nanosized TiO_2 particles are still scarce, especially the influence of HSs on the physicochemical behavior of Eu(III) on nanoparticles of TiO_2.

The study of Eu(III) adsorption onto TiO_2 is helpful and essential for the evaluation of trivalent lanthanides and actinides physicochemical behavior. The aims of the present study are (1) to study the effect of pH, concentration, ionic strength and fulvic acid (FA) on Eu(III) adsorption on TiO_2; (2) to study the influence of FA on Eu(III) adsorption onto TiO_2; (3) to determine the adsorption isotherms of Eu(III) to TiO_2; (4) to model the experimental data with the aid of FITEQL 3.2; (5) to identify the local species of Eu(III) adsorbed on TiO_2 surfaces and (6) to evaluate the adsorption mechanism of Eu(III) on TiO_2.

2. Materials and methods

2.1. Materials

Eu stock solution was prepared from Eu_2O_3 by dissolution, evaporation and redissolution in 10^{-3} mol/L perchloric acid. The radiotracer $^{152+154}$Eu(III) was used and the concentration was analyzed by liquid scintillation counting using a Packard 3100 TR/AB Liquid Scintillation analyzer (PerkinElmer). The scintillation cocktail was ULTIMA GOLD AB (Packard).

The sample of TiO_2 (P25, from Degussa Corporation) is composed of 80% anatase and 20% rutile (from the X-ray diffraction (XRD) result shown in Fig. 1). The specific surface area and surface site density values, as employed in the adsorption modeling, were 55 m^2/g and 2.74×10^{-4} mol/g [22], respectively. The pH_{pzc} of TiO_2 sample was measured to be 6.15 [24].
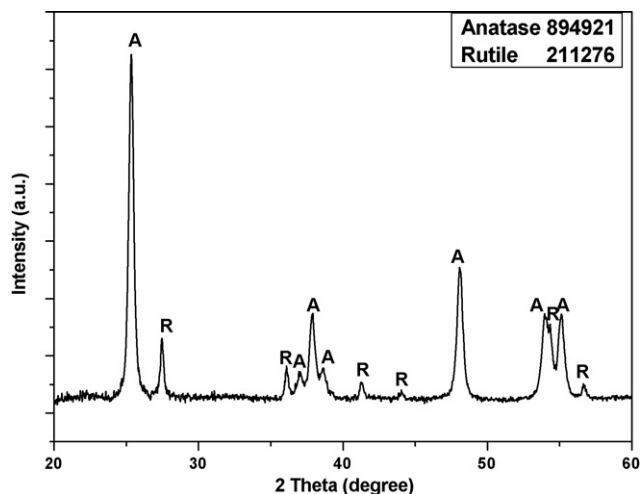
Fig. 1. The XRD pattern of P25 sample.

Table 1
^{13}C NMR characteristics (chemical shift ppm)% of FA.

HSs	0–50	51–105	106–160	161–200	Aromaticity
FA	16	28	19	39	30

Soil FA was extracted from the soil of Hua-Jia county (Gansu province, China), and has been characterized in detail [26,27]. Cross-polarization magic angle spinning (CPMAS) ^{13}C NMR spectra of FA was divided into four chemical shift regions, 0–50, 51–105, 106–160 and 161–200 ppm. These regions were referred to as aliphatic, carbohydrate, aromatic and carboxyl regions. The percentage of total intensity for each region is estimated by integrating the CPMAS ^{13}C NMR spectra with each region and the fraction of aromatic groups calculated by expressing aromatic C as percentage of the sum of aliphatic C (0–105 ppm) + aromatic C (106–160 ppm) is listed in Table 1.

2.2. Batch experiments

The adsorption of Eu(III) on TiO_2 particles was investigated by using batch technique under N_2 condition at $T = 20 \pm 2\,^{\circ}$C in 0.01 mol/L $NaClO_4$ solutions. All solutions were prepared using Milli-Q water, and all experiments were conducted in polyethylene tubes. The aqueous solution volume was adjusted with a solution containing background electrolyte $NaClO_4$, Eu(III), FA, TiO_2 and Milli-Q water. Soil FA was first equilibrated with TiO_2 suspension for 3 days, and then Eu(III) stock solution was added into FA–TiO_2 suspension to start the adsorption of Eu(III) on FA–TiO_2 hybrids. $HClO_4$ or NaOH were added to achieve the desired pH of the aqueous suspensions. The test tubes were shaken for 4 days to achieve the adsorption equilibration. Our pre-experiments demonstrated that 4 days were enough to achieve the equilibration of Eu(III) adsorption on TiO_2. For adsorption isotherms, the pH was maintained to 4.50 ± 0.05. After equilibration, the suspension was centrifuged at 18,000 rpm for 30 min at temperature controlled at 20 °C to separate the solid phase from the liquid one. The concentration of Eu(III) adsorbed on TiO_2, C_s (mol/g), was calculated from the difference of initial Eu(III) concentration (C_0) and final concentration remained in solution after equilibrium (C_{eq}), the volume of the solution (V) and the mass of TiO_2 (m) with the equation $C_s = (C_0 - C_{eq}) \times V/m$.

2.3. X-ray photoelectron spectroscopy (XPS) analysis

For spectroscopic analysis, adsorption experiments were conducted with 0.3 g/L TiO_2, 0.01 mol/L $NaClO_4$ and 3.0×10^{-5} mol/L Eu(III) at pH = 4.5 ± 0.1. The solid was separated by filtration and subsequently washed with 0.01 mol/L $NaClO_4$ solution to remove non-adsorbed Eu(III), and then the solid phases were dried under vacuum and ambient temperature. Only part of free water on solid phases was removed in this treatment, and this treatment did not result in any surface species modification. The XPS spectra were recorded on powders with a thermo ESCALAB 250 spectrometer using an Al Kα monochromator source and a multidetection analyzer, under a 10^{-8} Pa residual pressure. Surface charging effects were corrected with C 1s peak at 284.6 eV as a reference.

3. Results and discussion

3.1. SEM images of TiO_2 samples

The field-emission scanning electron microscopy (FE-SEM) was used to observe the changes in morphological features of TiO_2 before and after Eu(III) adsorption in the absence/presence of FA. From Fig. 2(c and d), it can be clearly seen that something appears on the boundary of TiO_2 particles comparing with Fig. 2(a and b).
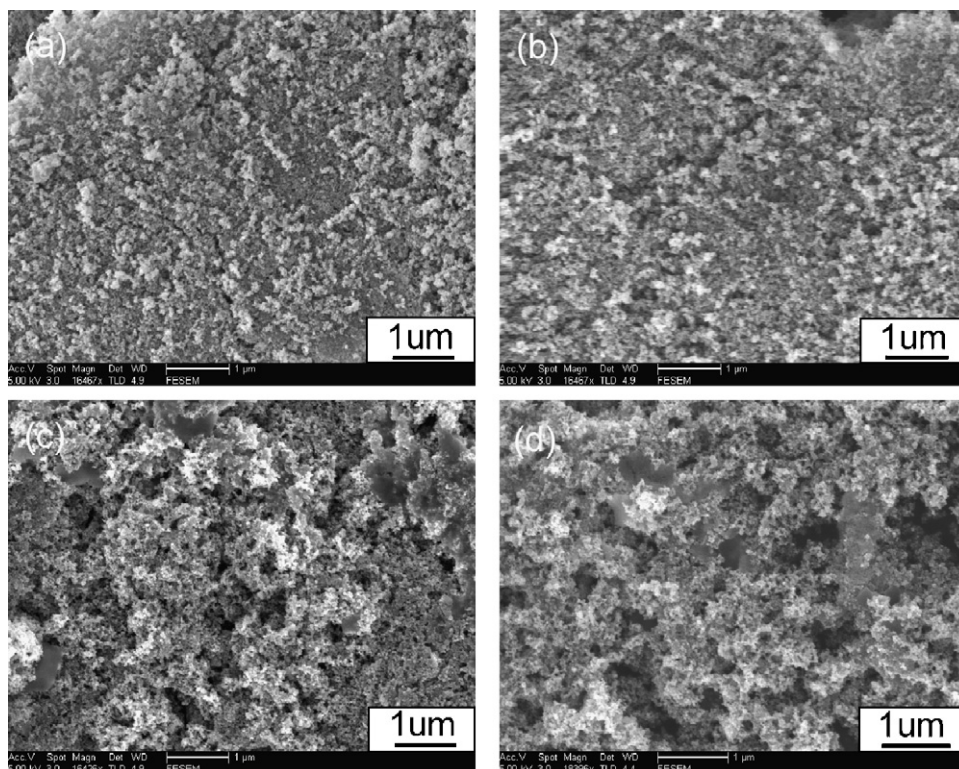
Fig. 2. SEM images of TiO$_2$ sample (a), Eu–TiO$_2$ (b), Eu–FA–TiO$_2$ (c) and (d).

This is attributed to the surface adsorbed FA on TiO$_2$ particles. The macromolecular structures of FA result in the obvious difference of SEM images of TiO$_2$ and FA–TiO$_2$ colloids. The SEM images indicate the difference of the microstructures and surface properties of TiO$_2$ and Eu–FA–TiO$_2$, which is attributed to the adsorption of Eu(III) and FA on TiO$_2$. After the adsorption of FA on TiO$_2$ particles, the macromolecular structures of FA attract TiO$_2$ particles together and thereby result in the aggregation of TiO$_2$ particles. So the sizes of FA–TiO$_2$ hybrids are bigger than those of pure TiO$_2$ particles.

3.2. Effect of pH on Eu(III) adsorption to bare TiO$_2$

Most of the investigations of metal ions' adsorption onto mineral surfaces published so far have confined to the pH-dependent adsorption (so called pH-edges) for one or two adsorbate concentrations. Fig. 3 shows the pH dependence of Eu(III) adsorption on bare TiO$_2$ in 0.01 mol/L NaClO$_4$ aqueous solutions at initial concentrations of Eu(III) 1.0×10^{-5}, 1.0×10^{-6} and 1.0×10^{-7} mol/L, respectively. As shown in Fig. 3, solution pH is the key factor to affect the adsorption of Eu(III) on TiO$_2$ particles. The adsorption of Eu(III) increases slowly at pH range 2–4, abruptly at pH 4–6, and at last maintains high level with increasing pH at pH > 6. About 99% of Eu(III) is adsorbed on TiO$_2$ at pH > 6. The strong pH-dependent adsorption suggests that Eu(III) adsorption is attributed to inner-sphere surface complexation rather than ion exchange or outer-sphere surface complexation. It is interesting to note that the adsorption edge of Eu(III) shifts to higher pH values with increasing Eu(III) initial concentrations. Similar pH-dependent results of Eu(III) adsorption on oxides were also observed by other researchers [3,5,6].

It is well known that the species of Eu(III) are crucial to Eu(III) adsorption. The species of Eu(III) are strongly dependent on pH value. The relative distribution of Eu(III) species in the aqueous solution calculated with the thermodynamic constants (Table 2) is shown in Fig. 4. It is clear that Eu^{3+} and Eu(OH)$^{2+}$ are the main
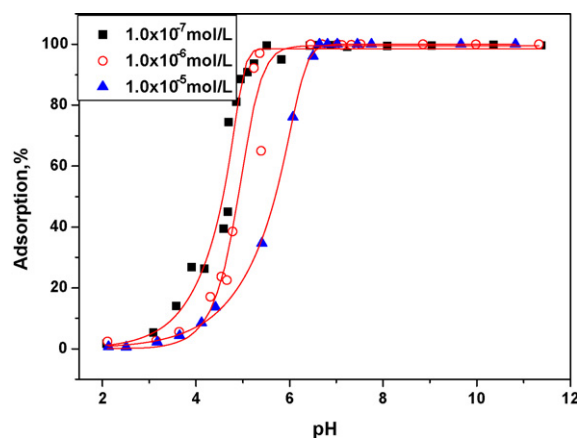

Fig. 3. Effect of pH on the adsorption of Eu(III) on bare TiO$_2$. $T = 20 \pm 2\,^\circ$C, $I = 0.01$ mol/L NaClO$_4$, $m/V = 0.3$ g (TiO$_2$)/L, $C_{Eu(III)initial} = 1.0 \times 10^{-5}$, 1.0×10^{-6}, 1.0×10^{-7} mol/L.

species of Eu(III) in solution at pH < 6.15 (i.e., pH$_{pzc}$), the free ≡SOH$_2^+$ and ≡SOH groups are the primary hydroxyl groups [28]. The adsorption of Eu^{3+} and Eu(OH)$^{2+}$ is unfavorable due to the coulombic repulsion. While, the positively charged Eu^{3+} or Eu(OH)$^{2+}$ species in solution may exchange with –H from hydroxyl groups, and the

Table 2
Aqueous thermodynamic data ($I = 0.01$ M NaClO$_4$; $T = 293.15$ K) used in the Eu modeling studies on TiO$_2$ (thermodynamic data taken from Wang et al. [3]).

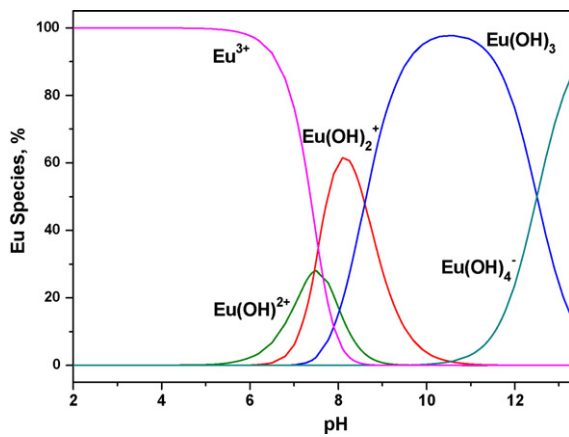| Reaction	Log K
H$_2$O ⇔ OH$^-$ + H$^+$	−13.79
Eu^{3+} + H$_2$O ⇔ Eu(OH)$^{2+}$ + H$^+$	−7.64
Eu^{3+} + 2H$_2$O ⇔ [Eu(OH)$_2$]$^+$ + 2H$^+$	−15.1
Eu^{3+} + 3H$_2$O ⇔ [Eu(OH)$_3$]^0 + 3H$^+$	−23.7
Eu^{3+} + 4H$_2$O ⇔ [Eu(OH)$_4$]$^-$ + 4H$^+$	−36.2

Fig. 4. Distribution of hydrolysis products of Eu(III) in aqueous solution.

increase in free hydroxyls concentration is the cause of the steep rise of Eu(III) adsorption. Thereby, the abrupt increase of adsorption does not correspond with the formation of hydrolysis of Eu(III) in solution, but rather due to the strong surface complexation [3]. While at higher pH values, the precipitation of Eu(III) may contribute to the adsorption.

Various SCMs have been developed and applied to simulate the adsorption of metal ions on oxides. The commonly adopted forms include the constant capacitance model (CCM), the diffusion layer model (DLM) and the triple layer model (TLM). Herein, the adsorption data are fitted using the DLM with the aid of FITEQL 3.2 code. On the basis of the complexation reactions and the corresponding equilibrium constants in Table 3, the surface species of Eu(III) adsorbed on TiO$_2$ as a function of pH is shown in Fig. 5. Clearly, the model simulates the experimental data very well. From Fig. 5, one can see that Eu(III) adsorbed on TiO$_2$ surface mainly presents as: $\equiv$SOEu^{2+} is the dominant specie at low pH values, $\equiv$SOEu(OH)$^+$ becomes the major species with increasing pH and $\equiv$SOEu(OH)$_2$ is the most abundant surface species at high pH values. This is in agreement with the relative species of Eu(III) in solution shown in Fig. 4. The WSOS/DF = 3.26×10^{-5}, 5.84×10^{-3}, 9.25×10^{-3} are obtained by fitting the Eu(III) adsorption on TiO$_2$, which indicates the satisfactory optimization procedure (Generally, WSOS/DF values in the range of 0–20 show a good fit of the data) [29].

3.3. Effect of pH on Eu(III) adsorption to bare and FA bound TiO$_2$

The pH dependence of Eu(III) adsorption on TiO$_2$ in the presence and absence of FA is shown in Fig. 6. The adsorption curve of Eu(III) on FA–TiO$_2$ hybrids shifts to the left as compared to that on bare TiO$_2$ at pH < 6, from which it can be concluded that the presence of FA enhances Eu(III) adsorption at pH < 6. FA has high content of oxygen due to the carboxyl and hydroxyl groups, which form strong complexes with metal ions [26,27]. The increase of Eu(III) adsorption on FA–TiO$_2$ hybrids is explained by the adsorption of FA on TiO$_2$ surface, followed by the strong complexation of Eu(III) with surface adsorbed FA on TiO$_2$ surfaces. This indicates that the complexation between FA and Eu(III) is stronger than that between
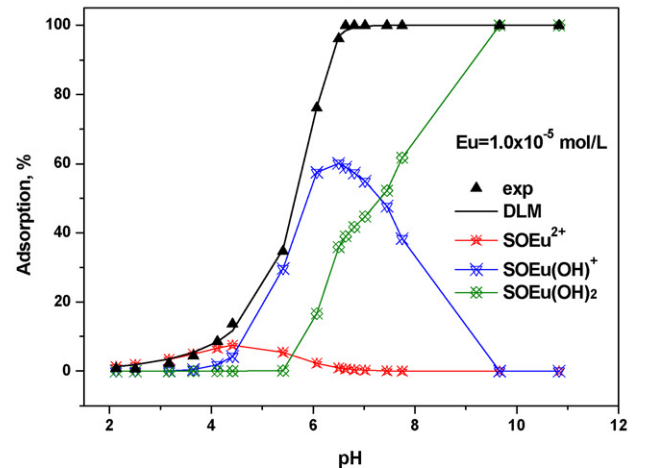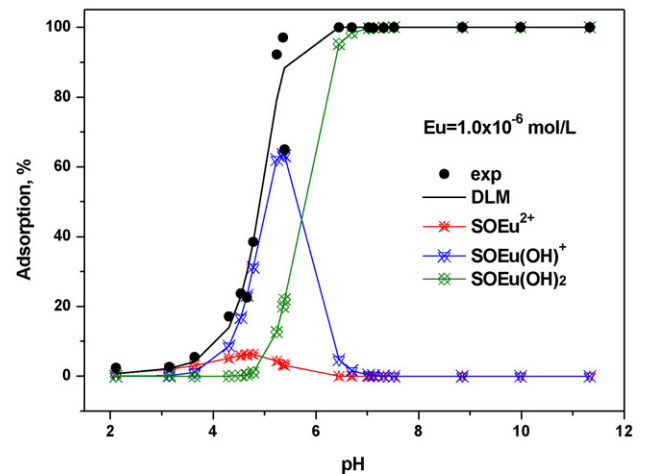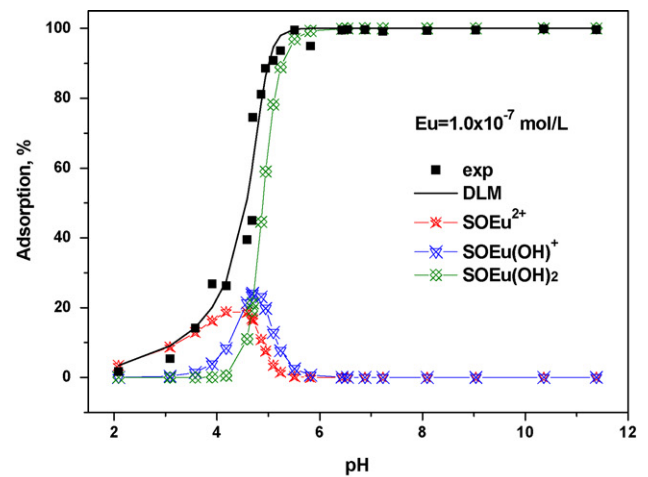
Fig. 5. Surface complex speciation repartition diagram of Eu(III) adsorption on TiO$_2$ as a function of pH at three different initial concentration.

Table 3
Surface complexation constants (pK_a) for Eu(III) adsorption on TiO$_2$ at different concentration.

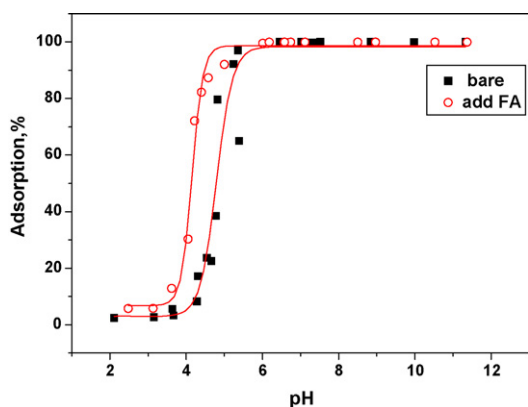|	1.0×10^{-7} mol/L Log K_a	1.0×10^{-6} mol/L Log K_a	1.0×10^{-5} mol/L Log K_a
$\equiv$SOH + Eu^{3+} $\Leftrightarrow$ $\equiv$SOEu^{2+} + H$^+$	−1.67	−2.37	−2.08
$\equiv$SOH + Eu^{3+} + H$_2$O $\Leftrightarrow$ $\equiv$SOEu(OH)$^+$ + 2H$^+$	−6.20	−6.45	−6.75
$\equiv$SOH + Eu^{3+} + 2H$_2$O $\Leftrightarrow$ $\equiv$SOEu(OH)$_2$ + 3H$^+$	−9.44	−11.18	−14.90
WSOS/DF	3.26×10^{-5}	5.84×10^{-3}	9.25×10^{-3}

Fig. 6. Effect of pH on the adsorption of Eu(III) on bare, FA bound TiO$_2$. $T = 20 \pm 2\,^\circ$C, $I = 0.01$ mol/L NaClO$_4$, $m/V = 0.3$ g (TiO$_2$)/L, C(FA)$_{initial} = 7.5$ mg/L, $C_{Eu(III)initial} = 1.0 \times 10^{-6}$ mol/L.

TiO$_2$ and Eu(III) [3,4]. At low pH values, the negatively charged HSs are easily to be adsorbed on positively surface charged oxides, and the strong complexation of metal ions with HSs adsorbed on oxides results in the increase of metal ion adsorption on HSs bound oxides. The adsorption of metal ions on HSs bound oxides is dominated by the nature of HSs, the nature of metal ions, the nature of solid particles, pH, ionic strength, and temperature etc. [28,30].

3.4. Effect of ionic strength on Eu(III) adsorption to bare and FA bound TiO$_2$

Fig. 7 shows the adsorption of Eu(III) on TiO$_2$ as a function of ionic strength at pH 4.30 ± 0.05. Within the experimental uncertainties, the adsorption of Eu(III) on TiO$_2$ is independent of ionic strength in the range of 0–0.2 mol/L NaClO$_4$. It is well known that ClO$_4^-$ does not form complexes with Eu(III) in solution, the influence of NaClO$_4$ is only attributed to the competition of Na$^+$ in the system. The ionic strength independent of Eu(III) adsorption suggests that the formation of strong inner-sphere surface complexes even under conditions where the net surface charge of TiO$_2$ is positive (pH$_{pzc}$ = 6.15). This indicates that the influence of surface potential on the adsorption reaction is of minor importance for the metal ions of high charge ($z \geq 3+$) [6]. The ion exchange does not contribute to the adsorption of Eu(III) on TiO$_2$. The results are also in agreement with the DLM modeling in Fig. 4. The uptake of metal ions in the adsorption edges, which exhibits a strong
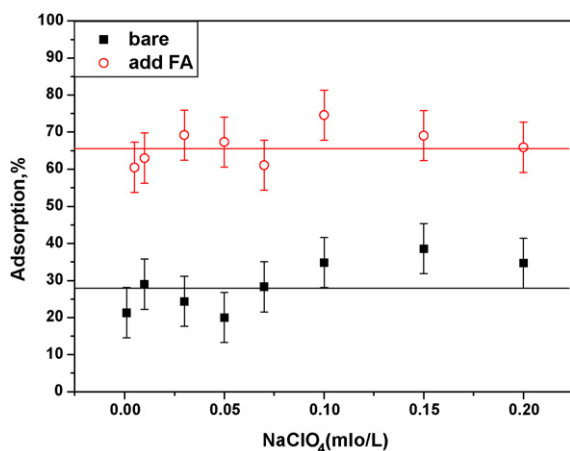

Fig. 7. Effect of ionic strength on Eu(III) adsorption to bare, FA bound TiO$_2$ particles. $T = 20 \pm 2\,^\circ$C, $m/V = 0.3$ g (TiO$_2$)/L, pH = 4.30 ± 0.05, C(FA)$_{initial} = 7.5$ mg/L, $C_{Eu(III)initial} = 1.0 \times 10^{-6}$ mol/L.
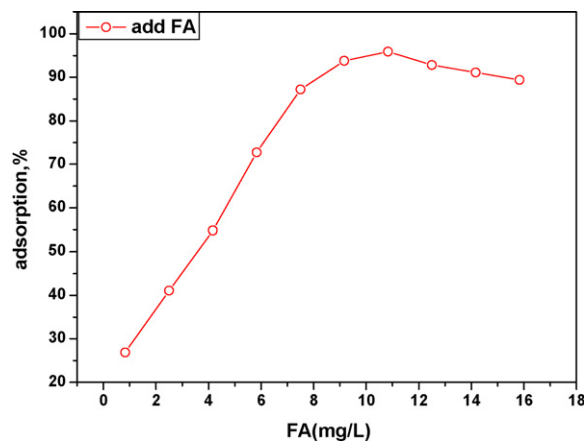

Fig. 8. Effect of FA concentration on Eu(III) adsorption to FA bound TiO$_2$ particles. $T = 20 \pm 2\,^\circ$C, $I = 0.01$ mol/L NaClO$_4$, $m/V = 0.3$ g(TiO$_2$)/L, pH = 4.50 ± 0.05, $C_{Eu(III)initial} = 1.0 \times 10^{-6}$ mol/L.

dependency on pH and weak dependency on ionic strength, is consistent with inner-sphere surface complexation. The results of this work are identical to those derived by Wang et al. [3] and Rabung et al. [6], although different samples of oxides were investigated.

3.5. Effect of FA concentrations on Eu(III) adsorption

Fig. 8 shows the removal percentage of Eu(III) from solution to FA–TiO$_2$ hybrids as a function of FA initial concentrations at pH 4.50 ± 0.05 in 0.01 mol/L NaClO$_4$ solutions. At this pH, the surface charge of TiO$_2$ is positive and the negatively charged FA is easily adsorbed on the surface of TiO$_2$. Adsorption percentage of Eu(III) on solid phases increases with increasing FA concentration in the ternary system, which indicates that the surface complexation of Eu(III) with surface adsorbed FA is stronger than that of Eu(III) with TiO$_2$ surface functional groups. With increasing FA concentration, more FA macromolecules are adsorbed on TiO$_2$ surfaces, and the surface adsorbed FA thereby provides more functional groups to bind Eu(III). At FA concentrations higher than 10.9 mg/L, the Eu(III) adsorption decreases with increasing FA concentration. From the result of acid–base titration of FA [31], the surface site density of FA is 2.71×10^{-2} mol/g. The surface site density of TiO$_2$ is 2.74×10^{-4} mol/g. Considering the concentrations of FA and TiO$_2$ in the system, the surface site concentration of TiO$_2$ in the system is 8.22×10^{-5} mol/L (i.e., 0.3 g/L $\times$ 2.74×10^{-4} mol/g). If all the surface sites of FA can form mono-surface complexes with TiO$_2$, 3 mg/L FA is enough to form the saturation adsorption of FA on TiO$_2$ surfaces. However, only fraction of functional groups of FA forms complexes on TiO$_2$ surfaces. With increasing FA concentrations, the percent of FA adsorbed on TiO$_2$ decreases and the percent of FA remained in solution increases. The effect of FA concentration on Eu(III) adsorption is attributable to the competition for Eu(III) between the FA in solution and the FA adsorbed on the mineral surfaces [32]. At C(FA)$_{initial}$ > 10.9 mg/L, the surface of the mineral is saturated with FA, the more the concentration of FA presents, the more the free FA macromolecules present in solution and the more efficient is the screening of the mineral surface. Under these conditions, the Eu(III) is more predominately in solution as Eu(III)–FA complexes. Thereby, the adsorption of Eu(III) decrease with increasing FA concentration at high FA concentrations.

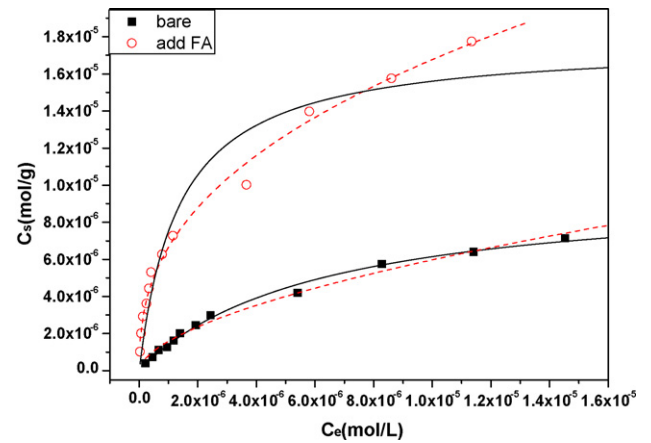### 3.6. Adsorption isotherms of Eu(III) on bare and FA bound TiO₂

Adsorption isotherms of Eu(III) on bare and FA bound TiO₂ particles are studied at pH 4.50 ± 0.05 in 0.01 mol/L NaClO₄ solutions (Fig. 9). Adsorption isotherm of Eu(III) on FA–TiO₂ hybrids is much higher than that of Eu(III) on bare TiO₂ particles, indicating that the adsorption of Eu(III) on FA–TiO₂ hybrids is higher than that of Eu(III) on bare TiO₂. This is in agreement with the results shown in Fig. 6. In order to gain a better understanding of the mechanism and to quantify the adsorption data, two models, the Langmuir and Freundlich isotherm models, are adopted to simulate the results.

The Langmuir model is widely used for modeling equilibrium data [33]. The isotherm is valid for monolayer adsorption onto a surface containing finite number of identical sites. It can be described by the equation:

$$C_s = \frac{K_a q_{max} C_{eq}}{1 + b C_{eq}} \tag{1}$$

where C_{eq} is the concentration of Eu(III) in solution at equilibration, C_s is the amount of Eu(III) adsorbed to form a monolayer coverage on the adsorbent particle, and K_a is the Langmuir adsorption equilibrium constant.

The Freundlich expression is an empirical equation describing adsorption onto heterogeneous surface [34]. The isotherm assumes

Fig. 9. Adsorption isotherms of Eu(III) on bare, FA bound TiO₂ particles. $T = 20 \pm 2\,°C$, $I = 0.01$ mol/L NaClO₄, $C(FA)_{initial} = 7.5$ mg/L, $m/V = 0.3$ g(TiO₂)/L, pH = 4.50 ± 0.05. Solid line: Langmuir model; dash line: Freundlich model.
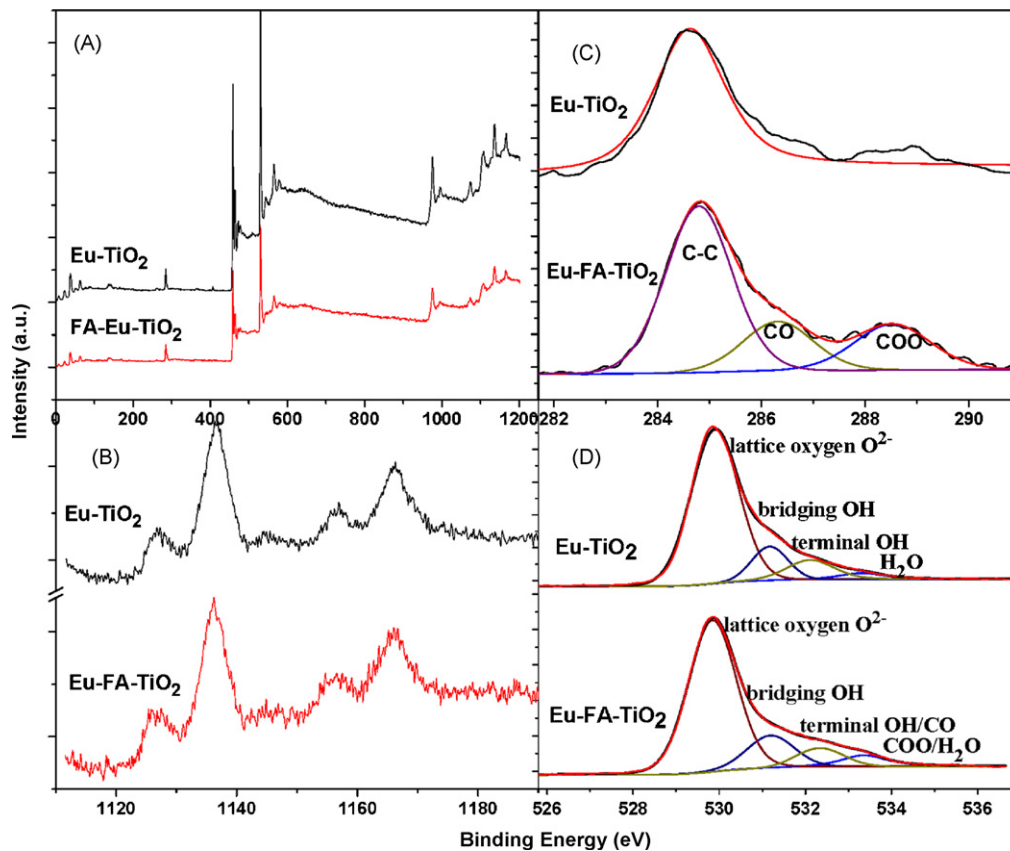
that the surface sites of the adsorbent have a spectrum of different binding energies. The equation is presented as:

$$C_s = k_F C_{eq}^{1/n} \tag{2}$$

Table 4
Parameter of adsorption models for Eu(III) on TiO₂.

System	Langmuir model			Freundlich model		
	q_{max} (mmol/g)	K_a (L/mmol)	R^2	K_F (mmol/g)	n	R^2
Bare	0.00991	163.3	0.9944	4.7	1.73	0.9896
Add FA	0.01773	733.7	0.9412	1.7	2.49	0.9922

Fig. 10. XPS spectra of survey (A), Eu 3d (B), C 1s (C) and O 1s (D) of Eu–TiO₂ and Eu–FA–TiO₂. $T = 20 \pm 2\,°C$, $I = 0.01$ mol/L NaClO₄, $m/V = 0.3$ g (TiO₂)/L, pH = 4.50 ± 0.05, $C(FA)_{initial} = 7.5$ mg/L, $C_{Eu(III)initial} = 1.0 \times 10^{-5}$ mol/L.

where K_F (mmol/g) is the adsorption capacity. The value of n indicates a favorable adsorption at $1 < n < 10$.

The Langmuir and Freundlich constants obtained by fitting the adsorption equilibrium data are listed in Table 4. The results indicate that the Langmuir model and the Freundlich model fit the adsorption well of Eu(III) onto bare TiO$_2$. However, the adsorption of Eu(III) onto TiO$_2$ in the presence of FA is poorly fitted by the Langmuir model compared with the Freundlich model. This means the adsorption behavior of Eu(III) is very complicated and might be affected by many factors in the presence of FA. The value of q_{max} obtained from the Langmuir model for Eu(III) adsorption on FA bound TiO$_2$ is higher than that on bare TiO$_2$, which indicates that the functional groups on the surfaces of FA–TiO$_2$ hybrids have a relatively stronger affinity for Eu(III) than those on bare TiO$_2$ surface. In the Freundlich model, the value of n is higher than unity, which indicates that metal ions are favorably adsorbed by TiO$_2$.

3.7. XPS analysis

In order to achieve the molecular level information of Eu(III) adsorbed on TiO$_2$, XPS (Fig. 10(A)) was used to identify the local species of Eu(III) adsorbed on TiO$_2$. The high resolution XPS Eu 3d spectra are shown in Fig. 10(B). The data leave no doubt that Eu(III) is chemically present within the near-surface of TiO$_2$ due to the adsorption. The XPS features of Eu 3d$_{5/2}$ at 1136 eV and Eu 3d$_{3/2}$ at 1166 eV in the samples, with a peak separation of 30 eV between the two peaks, are associated with inner-sphere surface complexes of Eu(III). The high resolution XPS C 1s spectra of the Eu–FA–TiO$_2$ and Eu–TiO$_2$ samples are shown in Fig. 10(C). The high resolution XPS C 1s spectrum of Eu–FA–TiO$_2$ hybrids is resolved into three individual component peaks: C–C (284.79 eV), CO (286.32 eV) and COO (288.52 eV), which indicates that the functional groups of FA are introduced in the TiO$_2$.

The Eu–TiO$_2$ sample has four O 1s peaks positioned at 529.9, 531.2, 532.2 and 533.3 eV (Fig. 10(D)), which can be assigned to lattice oxygen O^{2-}, bridging OH, terminal OH and adsorbed H$_2$O, respectively [35]. The OH attributes greatly to the sorption of Eu(III) on TiO$_2$ surface. While in the Eu–FA–TiO$_2$ sample, the O 1s spectrum is also deconvoluted into four peaks. The relative intensity of peak at 531.2 eV decreases, while the relative intensities of peaks at 532.2 and 533.3 eV increase. The increased peaks can also be assigned to other oxygen species, CO (532.2 eV) and COO (533.3 eV) [36], which are more easily to complex with Eu(III). Anyway, the positions of the O 1s peaks from the Eu–TiO$_2$ system are nevertheless different from those of the Eu–FA–TiO$_2$. The functional groups of FA at the TiO$_2$ surfaces contribute to Eu(III) adsorption (as explained in the previous part).

4. Conclusion

The adsorption of Eu(III) on TiO$_2$ is strongly dependent on pH values and independent of ionic strength, indicating that inner-sphere surface complexation is the main adsorption mechanism. The presence of FA enhances the adsorption of Eu(III) on TiO$_2$ at low pH values. The competition between the complexation of adsorbed FA and the soluble FA in solution with Eu(III) can explain the observations of Eu(III) adsorption on FA–TiO$_2$ hybrids. The Eu(III) adsorbed on TiO$_2$ can be assumed in the form of inner-sphere surface complexes of $\equiv$SOEu^{2+}, $\equiv$SOEu(OH)$^+$ and $\equiv$SOEu(OH)$_2$. The experimental data can be simulated well with DLM with the aid of FITEQL 3.2 mode. The batch and XPS results indicate the same/similar species and mechanism of Eu(III) adsorption on TiO$_2$ surface. The results are important to understand the adsorption of trivalent lanthanides/actinides in the environment.

References

[1] A.J. Fairhurst, P. Warwick, S. Richardson, The influence of humic acid on the sorption of europium onto inorganic colloids as a function of pH, Colloids Surf. A 99 (1995) 187–199.
[2] D. Xu, Q.L. Ning, X. Zhou, C.L. Chen, A.D. Wu, X.K. Wang, Sorption and desorption of Eu(III) on alumina, J. Radioanal. Nucl. Chem. 266 (2005) 419–424.
[3] X. Wang, D. Xu, L. Chen, X. Tan, X. Zhou, A. Ren, Ch. Chen, Sorption and complexation of Eu(III) on alumina: effect of pH, ionic strength, humic acid and chelating resin on kinetic dissociation study, Appl. Radiat. Isot. 64 (2006) 414–421.
[4] W.M. Dong, X.K. Wang, X.Y. Bian, A.X. Wang, J.Z. Du, Z.Y. Tao, Comparative study on sorption/desorption of radioeuropium on alumina, bentonite and red earth: effects of pH, ionic strength, fulvic acid, and iron oxides in red earth, Appl. Radiat. Isot 54 (2001) 603–610.
[5] A. Naveau, F. Monteil-Rivera, J. Dumonceau, S. Boudesocque, Sorption of europium on a goethite surface: influence of background electrolyte, J. Contam. Hydrol. 77 (2005) 1–16.
[6] Th. Rabung, Th. Stumpf, H. Geckeis, R. Klenze, J.I. Kim, Sorption of Am(III) and Eu(III) onto γ-alumina: experiment and modeling, Radiochim. Acta 88 (2000) 711–716.
[7] M.H. Bradbury, B. Baeyens, Experimental measurements and modeling of sorption competition on montmorillonite, Geochim. Cosmochim. Acta 69 (2005) 4187–4197.
[8] V.A. Sinitsyn, S.U. Aja, D.A. Kulik, S.A. Wood, Acid–base surface chemical and sorption of some lanthanides on K$^+$-saturated Marblehead illite: I. Result of an experimental investigation, Geochim. Cosmochim. Acta 64 (2000) 185–194.
[9] T. Rabung, H. Geckeis, J. Kim, H.P. Beck, Sorption of Eu(III) on a natural hematite: application of a surface complexation model, J. Colloid Interf. Sci. 208 (1998) 153–161.
[10] M.H. Bradbury, B. Baeyens, Sorption of Eu on Na- and Ca-montmorillonites: experimental investigation and modeling with cation exchange and surface complexation, Geochim. Cosmochim. Acta 66 (2002) 2325–2334.
[11] G. Montavon, T. Rabung, H. Geckeis, B. Grambow, Interaction of Eu(III)/Cm(III) with alumina-bound poly(acrylic acid): sorption, desorption, and spectroscopic studies, Environ. Sci. Technol. 38 (2004) 4312–4318.
[12] Th. Rabung, M.C. Pierret, A. Bauer, H. Geckeis, M.H. Bradbury, B. Baeyens, Sorption of Eu(III)/Cm(III) on Ca-montmorillonite and Na-illite. Part I: batch sorption and time-resolved laser fluorescence spectroscopy experiments, Geochim. Cosmochim. Acta 69 (2005) 5393–5402.
[13] Y. Takahashi, T. Kimura, Y. Kato, Y. Minai, Speciation of europium sorbed on a montmorillonite surface in the presence of polycarboxylic acid by laser-induced fluorescence spectroscopy, Environ. Sci. Technol. 33 (1999) 4016–4021.
[14] M.L. Schlegel, I. Pointeau, N. Coreau, P. Reiller, Mechanism of europium retention by calcium silicate hydrates: an EXAFS study, Environ. Sci. Technol. 38 (2004) 4423–4431.
[15] Th. Stumpf, A. Bauer, F. Coppin, Th. Fanghänel, J.I. Kim, Inner-sphere, outer-sphere and ternary surface complexes: a TRLFS study of the sorption process of Eu(III) onto smectite and kaolinite, Radiochim. Acta 90 (2002) 345–349.
[16] J.R. Lead, J. Hamilton-Taylor, A. Peters, S. Reiner, E. Tipping, Europium binding by fulvic acids, Anal. Chim. Acta 369 (1998) 171–180.
[17] D.G. Kinniburgh, C.J. Milne, M.F. Benedetti, J.P. Pinheiro, J. Filius, L.K. Koopal, et al., Metal ion binding by humic acid: application of the NICA-Donnan model, Environ. Sci. Technol. 30 (1996) 1687–1698.
[18] A.M. Jakobsson, Measurement and modeling of Th sorption onto TiO$_2$, J. Colloid Interf. Sci. 220 (1999) 367–373.
[19] M.S. Kim, K.M. Hong, J.G. Chung, Removal of Cu from aqueous solutions by adsorption process with anatase-type titanium dioxide, Water Res. 37 (2003) 3524–3529.
[20] P.A. O'Day, C.J. Chrisholm-Brause, S.N. Towle, G.A. Parks, G.E. Brown Jr., X-ray absorption spectroscopy of Co(II) sorption complexes on quartz (α-SiO$_2$) and rutile (TiO$_2$), Geochim. Cosmochim. Acta 60 (1996) 2432–2515.
[21] K.P. Saripalli, B.P. McGrail, D.C. Girvin, Adsorption of molybdenum on to anatase from dilute aqueous solutions, Appl. Geochem. 17 (2002) 649–656.
[22] M.S. Vohra, A.P. Davis, Adsorption of Pb(II), NTA, and Pb(II)–NTA onto TiO$_2$, J. Colloid Interf. Sci. 194 (1997) 59–67.
[23] C.S. Uyguner, M. Bekbolet, Evaluation of humic acid, chromium(VI) and TiO$_2$ ternary system in relation to adsorptive interactions, Appl. Catal. B 49 (2004) 267–275.
[24] C.H. Weng, J.H. Wang, C.P. Huang, Adsorption of Cr(VI) onto TiO$_2$ from dilute aqueous solutions, Water Sci. Tech. 35 (1997) 55–62.
[25] M. Olsson, A.M. Jakobsson, Y. Albinsson, Sorption of Pu(VI) onto TiO$_2$, J. Colloid Interf. Sci 266 (2003) 269–275.
[26] Z.Y. Tao, J. Zhang, J. Zhai, Characterization and differentiation of humic acids and fulvic acids in soils from various regions of China by nuclear magnetic resonance spectroscopy, Anal. Chim. Acta 395 (1999) 199–203.
[27] J. Zhang, J.J. Zhai, F.Z. Zhao, Z.Y. Tao, Study of soil humic substances by cross-polarization magic angle spinning ^{13}C nuclear magnetic resonance and pyrolysis-capillary gas chromatography, Anal. Chim. Acta 378 (1999) 177–182.

[28] X. Tan, X. Wang, M. Fang, C. Chen, Sorption and desorption of Th(IV) on nanoparticles of anatase studied by batch and spectroscopy methods, Colloids Surf. A 296 (2007) 109–116.

[29] A.L. Heberlin, J.C. Westall, FITEQL: A computer program for determination of equilibrium constants from experimental data, Version 3.2, Report 96-01, Department of Chemistry, Oregon State University, 1996.

[30] C.L. Chen, X.K. Wang, Influence of pH, soil humic/fulvic acid, ionic strength and foreign ions on sorption of thorium(IV) onto γ-Al_2O_3, Appl. Geochem. 22 (2007) 436–445.

[31] X.L. Tan, X.K. Wang, H. Geckeis, Th Rabung, Sorption of Eu(III) on humic acid or fulvic bound to hydrous alumina studied by SEM-EDS, XPS,TRLFS, and batch techniques, Environ. Sci. Technol. 42 (2008) 6532–6537.

[32] Y. Wan, C. Liu, The effect of humic acid on the adsorption of REE on Kaolin, Colloids Surf. A 290 (2006) 112–117.

[33] I. Langmuir, The adsorption of gases on plane surfaces of glass, mica and platinum, J. Am. Chem. Soc. 40 (1918) 1361–1403.

[34] H.M.F. Freundlich, Uber die adsorption in lasungen, J. Phys. Chem. 57 (1906) 385–470.

[35] P.L. Cao, D.E. Ellis, V.P. Dravid, First-principles study of initial stage of Ni thin-film growth on a TiO_2 (1 1 0) surface, J. Mater. Res. 14 (1999) 3684–3689.

[36] H. Wang, A. Zhou, F. Peng, H. Yu, J. Yang, Mechanism study on adsorption of acidified multiwalled carbon nanotubes to Pb(II), J. Colloid Interf. Sci. 316 (2007) 277–283.